JACS
JOURNAL OF THE AMERICAN CHEMICAL SOCIETY
Communication
pubs.acs.org/JACS

Blurring the Role of Oligonucleotides: Spherical Nucleic Acids as a Drug Delivery Vehicle

Xuyu Tan, Xueguang Lu, Fei Jia, Xiaofan Liu, Yehui Sun, Jessica K. Logan, and Ke Zhang*

Department of Chemistry and Chemical Biology, Northeastern University, Boston, Massachusetts 02115, United States

Supporting Information

ABSTRACT: Nucleic acids are generally regarded as the payload in gene therapy, often requiring a carrier for intracellular delivery. With the recent discovery that spherical nucleic acids enter cells rapidly, we demonstrate that nucleic acids also have the potential to act as a delivery vehicle. Herein, we report an amphiphilic DNA-paclitaxel conjugate, which forms stable micellar nanoparticles in solution. The nucleic acid component acts as both a therapeutic payload for intracellular gene regulation and the delivery vehicle for the drug component. A bioreductively activated, self-immolative disulfide linker is used to tether the drug, allowing free drug to be released upon cell uptake. We found that the DNA-paclitaxel nanostructures enter cells ~100 times faster than free DNA, exhibit increased stability against nuclease, and show nearly identical cytotoxicity as free drug. These nanostructures allow one to access a gene target and a drug target using only the payloads themselves, bypassing the need for a cocarrier system.

Carrier systems are commonly used to overcome intrinsic difficulties of drug molecules such as poor water solubility and stability, and facilitate delivery.[1] Carrier-drug conjugation is a method distinct from encapsulation that brings unique benefits such as consistent drug formulation and increased stability through covalent binding of two components.[2] In the last few decades, various drug conjugates, such as polymer-drug, peptide-drug, drug-drug, and antibody-drug conjugates, have been reported,[3] which achieve improved drug properties such as higher water solubility, longer blood circulation times, enhanced serum stability and cell uptake, and improved targeting.[4]

Among these conjugate systems, nucleic acid-drug conjugates (NADC) are highly versatile and yet relatively underexplored. Functional nucleic acid sequences such as siRNA and antisense oligonucleotides are powerful molecules to control cellular expression of individual proteins,[5] many of which lack small molecule inhibitors,[6] and can work together with drugs to address difficult challenges such as multidrug resistance.[7] However, nucleic acid themselves are too hydrophilic for passive diffusion into cells, and intracellular delivery typically requires electrostatic complexation with a polycationic carrier, which facilitates endocytosis.[8] For combination therapies requiring the codelivery of nucleic acids and hydrophobic drugs, modified polycationic carriers containing a hydrophobic pocket are a popular solution.[7] However, the complicated designs of these carriers and their potential toxic and immunogenic side effects put a brake on their rapid clinical adoption.[9]

The notion that a nucleic acid is a fragile molecule needing protection and is unable to enter cells suggests that it is preposterous to consider it as a delivery vehicle for other payloads. Nonetheless, the highly hydrophilic, nontoxic, and biodegradable characters of nucleic acids are all desirable properties of a carrier. Recently, it has been discovered that, by ordering oligonucleotides into a dense, spherical spatial arrangement (spherical nucleic acids, or SNAs), nucleic acids can engage in scavenger receptor-mediated endocytosis and be rapidly taken up by essentially all cell types other than red blood cells.[10] Such arrangement can also provide the oligonucleotides with many other properties such as improved nuclease stability, enhanced binding constant with a complementary sequence, and ability to permeate the skin.[11] These unique properties of SNAs have been found to arise from the arrangement of the oligonucleotides and are not affected by the core composition of the sphere.[12] These discoveries beg the reconsideration of nucleic acid's role from being a payload to being both a payload and a delivery vehicle.

Here, we report a drug-cored SNA, which exploits the opposing hydrophilicities of nucleic acids and the anticancer drug paclitaxel (PTX). By covalently joining the two payloads together, the amphiphilic NADC can self-assemble into micellar nanoparticles, which are structurally analogous to SNAs (Scheme 1). To control the ratio between the number of PTX and DNA molecules, the PTX is attached to a

Scheme 1. (A) Schematics for the Formation of DNA-PTX$_{10}$ Micelles and Their Intended Actions and (B) Molecular Structure of DNA-PTX$_{10}$ Amphiphile

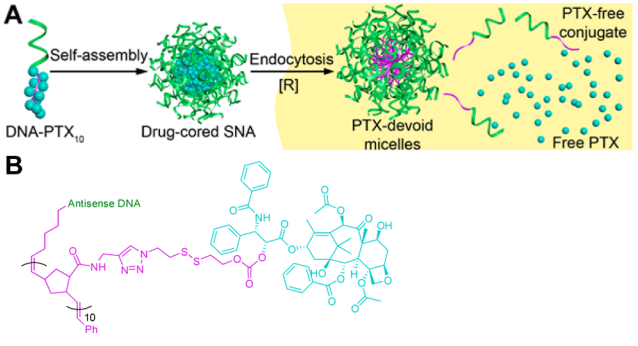

Received: July 21, 2016
Published: August 15, 2016

DOI: 10.1021/jacs.6b07554
J. Am. Chem. Soc. 2016, 138, 10834−10837

norbornenyl group and prepolymerized by ring-opening metathesis polymerization.[13] The polymerization is terminated with an azide-containing end-cap,[14] allowing for "clicking" of a single DNA strand.[15] The use of multiple PTX molecules per amphiphile also provides ample driving force for micellization, negating the need for divalent cations which facilitate micellization through screening of the repulsive interactions between DNA strands.[16]

We designed monomer 7, which consists of a PTX linked to a norbornenyl group via a bioreductively activated self-immolative linker (Scheme S1). The linker contains a disulfide bond, which can be cleaved under the reducing environment of the cell, to give a free sulfhydryl group that rapidly undergoes intramolecular cyclization with the adjacent carbonate to expel a free payload molecule.[17] Monomer 7 was synthesized in 5 steps with 20% overall yield (Scheme S1). Successful synthesis was confirmed by MALDI-ToF mass spectrometry (m/z = 1256.98 $[M + Na]^+$, calcd 1256.42, Figure S1). A degree of polymerization of 10 was chosen for balanced amphiphilicity with the DNA. The polymerization was terminated by adding aliquots of 6-azido-1-methoxyhex-1-ene, which places a single azide group at the ω-terminus of the PTX_{10} polymer. Gel permeation chromatography showed that the PTX_{10} polymer was narrowly dispersed (PDI = 1.2, M_w = 13 kDa, Figure S2).

For the DNA segment, we chose an antisense sequence (G3139) that targets the antiapoptotic B-cell lymphoma 2 (Bcl-2) family proteins as a proof-of-concept. The choice of target stems from the observation that the Bcl-2 protein is often responsible for chemotherapeutic resistance.[18] Furthermore, development of small molecule Bcl-2 inhibitors with suitable pharmacologic properties has proven to be difficult.[19] A fluorescein reporter and a dibenzocyclooctyne group were incorporated in the strand to enable tracking and conjugation with the PTX_{10} polymer, respectively. The click coupling was performed in DMSO:water mixture (9:1 v:v), and DNA-PTX_{10} was synthesized in 40% yield, as determined by band densitometry analysis (Figure S3).

The size of the DNA-PTX_{10} micelles was characterized by transmission electron microscopy (TEM) and dynamic light scattering (DLS). TEM clearly shows the formation of uniform spherical nanoparticles with a number-average diameter of 14.2 ± 2.7 nm (Figure 1A). The hydrodynamic diameter of the particles in water was determined to be 16.4 ± 6.4 nm (volume average) by DLS (Figure S4), consistent with TEM measurements. The DNA-PTX_{10} particles show a negative ζ-potential of −25.0 ± 3.2 mV in Nanopure water, as expected from the negatively charged DNA shell. The critical micelle concentration (CMC) of the DNA-PTX_{10} nanoparticles was determined by light scattering to be 97 nM in pure water, while the value in 1× PBS buffer was too low to be measured (Figure S5). This observation can be explained by the higher ionic strength of the PBS buffer, which produces a charge-screening effect, reducing the DNA−DNA repulsive interaction and leading to a reduction of the CMC to undetectable (<10 nM) levels. Therefore, the DNA-PTX_{10} micelles under physiological conditions can be considered as a pure particle system free of monomeric components.

Increased nuclease stability is critically important as degradation can occur both intracellularly and extracellularly, and only intact oligonucleotide reaching the cytosol of the cell can achieve the intended gene silencing effect.[20] To test the nuclease stability of DNA-PTX_{10} nanostructures, we adopted a literature method in which a quencher-labeled strand is

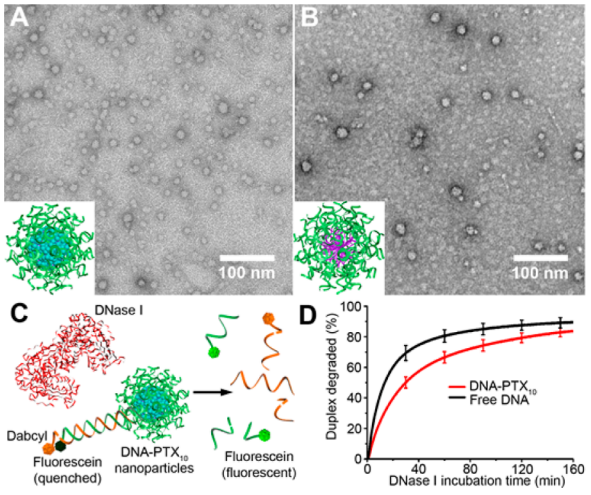

Figure 1. (A) and (B) TEM images of the DNA-PTX_{10} and PTX-devoid nanoparticles, respectively. Samples were stained with uranyl acetate (2%). (C) Schematic representations of a nuclease stability assay. (D) Kinetics of the enzymatic degradation of DNA-PTX_{10} and free DNA duplexes (100 nM), expressed as fluorescence intensity as a function of time upon DNase I introduction.

hybridized to a fluorophore-labeled complementary strand.[21] Upon nuclease degradation, the fluorophore is separated from the quencher, leading to an increase in fluorescent signal. Using the endonuclease DNase I (0.5 unit in 1 mL DNase buffer) as a model nuclease, the kinetics of the enzymatic degradation was monitored (Figure 1C). The half-life of DNA-PTX_{10} is ∼2.3 times longer than that of free DNA (Figure 1D), consistent with typical SNA structures.[22]

To monitor the kinetics of payload release from DNA-PTX_{10} particles, reverse-phase HPLC and gel electrophoresis were used. In order to simulate the reducing intracellular environment, DNA-PTX_{10} nanoparticles were treated with 10 mM dithiothreitol (DTT) solution at 37 °C for different durations (0−8 h). The HPLC peak corresponding to the DNA-PTX_{10} conjugate decreased in intensity after DTT treatment, and a new peak associated with PTX-free conjugate arose (Figure 2A). The peak integrations were used to calculate the extent of PTX release. Interestingly, ∼80% of the conjugate was cleaved after only 1 h of incubation, and subsequent release of PTX was

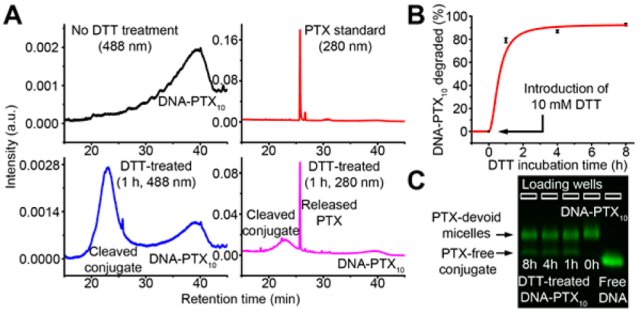

Figure 2. (A) Reverse-phase HPLC chromatograms of the DNA-PTX_{10} nanoparticles before (black) and after (blue and purple) 10 mM DTT treatment, showing the release of free PTX, which matches the retention time of standard PTX (red). (B) Drug release kinetics for the DNA-PTX_{10} nanoparticle as a function of DTT incubation times. (C) Agarose gel electrophoresis of free DNA, DNA-PTX_{10} nanoparticles, and nanoparticles treated with DTT for different times (1−8 h).

DOI: 10.1021/jacs.6b07554
J. Am. Chem. Soc. 2016, 138, 10834−10837

much slower, reaching 92% after 8 h (Figure 2B). The capability to burst-release inside the cell is a potentially advantageous property because it may increase the intracellular accumulation of the drug. The HPLC retention time of PTX released from conjugate and the molecular weight as determined by mass spectrometry matched that of free PTX were. Therefore, we conclude that the released PTX is in the free drug form as opposed to a pro-drug (Figure 2A).

Gel electrophoresis of DTT-treated DNA-PTX_{10} nanoparticles showed a new band that migrated faster than the intact micelles, correlating with the monomeric form of PTX-free conjugate that was separated from the micelle. Surprisingly, the major bands in all cases had the same migration rate as the untreated DNA-PTX_{10} nanostructures (Figure 2C). This implies that PTX-devoid conjugates are still able to retain the micelle structure because of the hydrophobic polymer component. It is also possible that the remaining free thiol groups on the polymer backbone can undergo disulfide exchange reactions to form cross-links, which covalently stabilize the micelles.[23] The major bands (PTX-devoid micelles) were isolated, purified by electroelution, and concentrated, and the resulting solution was subjected to prolonged DTT treatment (overnight). Gel electrophoresis showed that DTT treatment cannot disrupt the PTX-devoid micelles by breaking interchain disulfide linkages that may form, implying that these micellar structures are thermodynamically stable (Figure S7). DLS confirmed the presence of particles, showing a volume average hydrodynamic diameter of 19.2 ± 8.7 nm (Figure S4), and TEM showed that the particles were of a spherical morphology with an average diameter of 15.0 ± 2.6 nm (Figure 1B), similar to the intact DNA-PTX_{10} particles.

To quantitatively examine the extent of cell uptake, SK-OV-3 cells were treated with free DNA and DNA-PTX_{10} nanoparticles (20−1000 nM) for 4 h and were subsequently collected for flow cytometry analysis. Cells treated with free DNA exhibited little uptake even at 1000 nM, showing similar fluorescence levels as that of free cells. Strikingly, when cells were treated with DNA-PTX_{10} particles, signals increased ∼100-fold compared with free DNA (Figure 3A). The mean fluorescence signals were similar to that of cells treated with an identical dose of Lipofectamine2k-complexed DNA (1000 nM, Figure 3B). However, Lipofectamine2k produced a broad range of cells having varying levels of uptake, while DNA-PTX_{10} particles resulted in uniformly high cell uptake for all cells. Confocal microscopy of cells treated with 1000 nM DNA-PTX_{10} confirmed that the particles were internalized by the cell as opposed to being surface associated (Figure 3C), whereas cells treated with free DNA produced nearly no fluorescence signals.

After confirming the intracellular delivery of DNA-PTX_{10} nanoparticles, we next examined the *in vitro* efficacy of the two payloads upon cell internalization. MTT cytotoxicity assay showed that cells exhibited similar dose−response curves when treated with DNA-PTX_{10} particles or free PTX (1−10,000 nM equivalent PTX, Figure 4A), with IC_{50} values for free PTX and DNA-PTX_{10} being 41 nM and 59 nM, respectively, implying that free PTX is highly available to the cell upon particle endocytosis. Because the DNA-PTX_{10} particles are toxic to cells, they cannot be directly used to measure the antisense activity of the nanoparticle's G3139 sequence. Therefore, DTT was used to pretreat the particles to remove the drug component, resulting in a drug-free form of the micelle. SK-

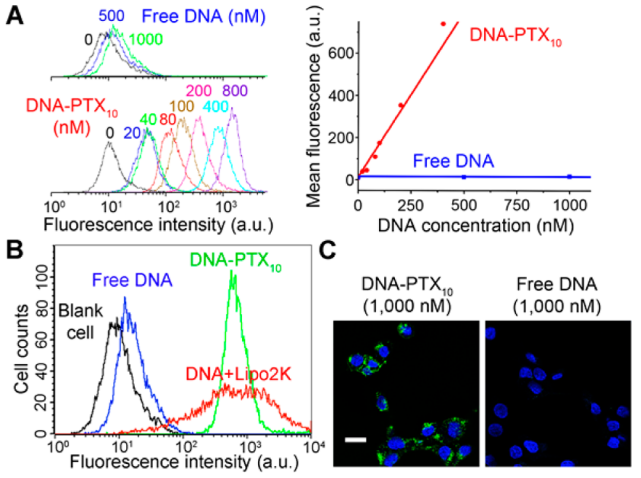

Figure 3. (A) Flow cytometry measurements (total cell counts: 10,000) of SK-OV-3 cells treated with varying concentrations of free DNA or DNA-PTX_{10} nanoparticles (0−1000 nM) for 4 h (left). The rate of cell uptake of DNA-PTX_{10} nanoparticles is ∼100 times faster than that of free DNA (right). (B) Flow cytometry measurements (total cell counts: 10,000) of SK-OV-3 cells treated with free DNA, DNA-PTX_{10} nanoparticles, and Lipofectamine2k-complexed DNA (4 h, 1000 nM DNA). (C) Confocal microscopy images of SK-OV-3 cells treated with DNA-PTX_{10} nanoparticles (left) and fluorescein-labeled free DNA (right) (4 h, 1000 nM DNA). Cell nuclei were stained with DAPI (blue). Images were taken under identical settings. Scale bar is 20 μm.

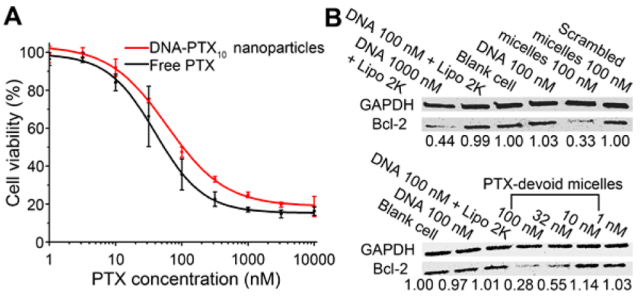

Figure 4. (A) MTT cytotoxicity assay of DNA-PTX_{10} nanoparticles and free PTX for SK-OV-3 cells, suggesting that the PTX component is readily available to the cell upon endocytosis. (B) Efficacy for antisense gene knockdown using PTX-devoid micelles, PTX-devoid micelles containing a scrambled sequence, Lipofectamine2k-complexed DNA, and free DNA (top) and dose response of PTX-devoid micelles (bottom).

OV-3 cells were treated with PTX-devoid micelles (1−100 nM), using Lipofectamine2k-complexed DNA as a positive control, and free DNA, PTX-devoid micelles containing a scrambled sequence with two base mismatches, and blank cells as negative controls. Western blot showed that cells treated with 100 nM PTX-devoid micelles have significantly reduced Bcl-2 expression (70% reduction), while 32 nM treatment achieved 45% reduction, as determined by band densitometry analysis. In contrast, 100 nM Lipofectamine2k-complexed DNA showed no decrease in Bcl-2 expression, and 56% decrease when the concentration was increased to 1000 nM. On the other hand, free DNA and PTX-devoid micelles containing the scrambled sequence resulted in similar levels of Bcl-2 expression as the blank cells (Figure 4B). Overall, *in vitro* studies demonstrate that DNA-PTX_{10} particles can enter cells in high quantities without a carrier system, and two payload

DOI: 10.1021/jacs.6b07554
J. Am. Chem. Soc. 2016, 138, 10834−10837

components can be activated by the cell and each carry out their intended functions.

In summary, we have synthesized a SNA-like DNA-drug nanostructure that can be bioreductively activated upon cell uptake. We have shown that oligonucleotides are an efficient carrier system for improving the water solubility of hydrophobic drugs and facilitating their intracellular delivery. The drug component allows for the conjugate to self-assemble into a dense, spherical form, which enables otherwise noncell-penetrating nucleic acids to undergo rapid endocytosis. Therefore, by covalently linking the two payloads together, disadvantages of the individual components can be transformed into useful properties. By taking advantage of intracellular reducing environment and self-immolative chemistry, free drugs can be accumulatively released from inside the cell, resulting in excellent retention of the drug's cytotoxicity. This self-assembled NADC bypasses the need for a complex carrier system that often give rise to additional cytotoxic or immunogenic challenges. With the recognition of the nucleic acid as both a vehicle and a payload, we anticipate that many more NADC structures will be developed to target a broad range of combination therapies.

■ ASSOCIATED CONTENT

Supporting Information

The Supporting Information is available free of charge on the ACS Publications website at DOI: 10.1021/jacs.6b07554.

Experimental details and data (PDF)

■ AUTHOR INFORMATION

Corresponding Author

*k.zhang@neu.edu

Notes

The authors declare no competing financial interest.

■ ACKNOWLEDGMENTS

We are grateful for Prof. George O'Doherty's support with cell culture. Financial support from Northeastern University startup, NEU-DFCI seed grant, and NSF CAREER award (1453255) is gratefully acknowledged.

■ REFERENCES

(1) (a) Yoo, J. W.; Irvine, D. J.; Discher, D. E.; Mitragotri, S. *Nat. Rev. Drug Discovery* **2011**, *10*, 521. (b) Tiwari, G.; Tiwari, R.; Sriwastawa, B.; Bhati, L.; Pandey, S.; Pandey, P.; Bannerjee, S. K. *Int. J. Pharm. Invest.* **2012**, *2*, 2.

(2) (a) Mitragotri, S.; Burke, P. A.; Langer, R. *Nat. Rev. Drug Discovery* **2014**, *13*, 655. (b) Luo, C.; Sun, J.; Sun, B.; He, Z. *Trends Pharmacol. Sci.* **2014**, *35*, 556.

(3) (a) Zou, J.; Zhang, F.; Zhang, S.; Pollack, S. F.; Elsabahy, M.; Fan, J.; Wooley, K. L. *Adv. Healthcare Mater.* **2014**, *3*, 441. (b) Liao, L.; Liu, J.; Dreaden, E. C.; Morton, S. W.; Shopsowitz, K. E.; Hammond, P. T.; Johnson, J. A. *J. Am. Chem. Soc.* **2014**, *136*, 5896. (c) Cheetham, A. G.; Zhang, P.; Lin, Y. A.; Lock, L. L.; Cui, H. *J. Am. Chem. Soc.* **2013**, *135*, 2907. (d) Su, H.; Zhang, P.; Cheetham, A. G.; Koo, J. M.; Lin, R.; Masood, A.; Schiapparelli, P.; Quinones-Hinojosa, A.; Cui, H. *Theranostics* **2016**, *6*, 1065. (e) Huang, P.; Wang, D.; Su, Y.; Huang, W.; Zhou, Y.; Cui, D.; Zhu, X.; Yan, D. *J. Am. Chem. Soc.* **2014**, *136*, 11748. (f) Falvo, E.; Tremante, E.; Fraioli, R.; Leonetti, C.; Zamparelli, C.; Boffi, A.; Morea, V.; Ceci, P.; Giacomini, P. *Nanoscale* **2013**, *5*, 12278.

(4) (a) Zhang, Y.; et al. *J. Mater. Chem. B* **2015**, *3*, 2472. (b) Zhou, Z.; Ma, X.; Jin, E.; Tang, J.; Sui, M.; Shen, Y.; Van Kirk, E. A.; Murdoch, W. J.; Radosz, M. *Biomaterials* **2013**, *34*, 5722. (c) Patterson, J. T.; Asano, S.; Li, X.; Rader, C.; Barbas, C. F. *Bioconjugate Chem.* **2014**, *25*, 1402. (d) Xiao, H.; Noble, G. T.; Stefanick, J. F.; Qi, R.; Kiziltepe, T.; Jing, X.; Bilgicer, B. *J. Controlled Release* **2014**, *173*, 11. (e) Huang, Y. F.; Shangguan, D.; Liu, H.; Phillips, J. A.; Zhang, X.; Chen, Y.; Tan, W. *ChemBioChem* **2009**, *10*, 862. (f) Callmann, C. E.; Barback, C. V.; Thompson, M. P.; Hall, D. J.; Mattrey, R. F.; Gianneschi, N. C. *Adv. Mater.* **2015**, *27*, 4611.

(5) (a) Carthew, R. W.; Sontheimer, E. J. *Cell* **2009**, *136*, 642. (b) Stein, C. A.; Cheng, Y. C. *Science* **1993**, *261*, 1004.

(6) Arkin, M. R.; Wells, J. A. *Nat. Rev. Drug Discovery* **2004**, *3*, 301.

(7) (a) Wang, Y.; Gao, S.; Ye, W. H.; Yoon, H. S.; Yang, Y. Y. *Nat. Mater.* **2006**, *5*, 791. (b) Li, J.; Wang, Y.; Zhu, Y.; Oupicky, D. *J. Controlled Release* **2013**, *172*, 589.

(8) (a) Kano, A.; Moriyama, K.; Yamano, T.; Nakamura, I.; Shimada, N.; Maruyama, A. *J. Controlled Release* **2011**, *149*, 2. (b) Meyer, M.; Philipp, A.; Oskuee, R.; Schmidt, C.; Wagner, E. *J. Am. Chem. Soc.* **2008**, *130*, 3272. (c) Luo, D.; Saltzman, W. M. *Nat. Biotechnol.* **2000**, *18*, 33.

(9) Ibricevic, A.; Guntsen, S. P.; Zhang, K.; Shrestha, R.; Liu, Y.; Sun, J. Y.; Welch, M. J.; Wooley, K. L.; Brody, S. L. *Nanomedicine* **2013**, *9*, 912.

(10) (a) Cutler, J. I.; Auyeung, E.; Mirkin, C. A. *J. Am. Chem. Soc.* **2012**, *134*, 1376. (b) Choi, C. H.; Hao, L.; Narayan, S. P.; Auyeung, E.; Mirkin, C. A. *Proc. Natl. Acad. Sci. U. S. A.* **2013**, *110*, 7625. (c) Giljohann, D. A.; Seferos, D. S.; Patel, P. C.; Millstone, J. E.; Rosi, N. L.; Mirkin, C. A. *Nano Lett.* **2007**, *7*, 3818.

(11) (a) Seferos, D. S.; Prigodich, A. E.; Giljohann, D. A.; Patel, P. C.; Mirkin, C. A. *Nano Lett.* **2009**, *9*, 308. (b) Lytton-Jean, A. K.; Mirkin, C. A. *J. Am. Chem. Soc.* **2005**, *127*, 12754. (c) Zheng, D.; Giljohann, D. A.; Chen, D. L.; Massich, M. D.; Wang, X. Q.; Iordanov, H.; Mirkin, C. A.; Paller, A. S. *Proc. Natl. Acad. Sci. U. S. A.* **2012**, *109*, 11975.

(12) Cutler, J. I.; Zhang, K.; Zheng, D.; Auyeung, E.; Prigodich, A. E.; Mirkin, C. A. *J. Am. Chem. Soc.* **2011**, *133*, 9254.

(13) Lu, X.; Watts, E.; Jia, F.; Tan, X.; Zhang, K. *J. Am. Chem. Soc.* **2014**, *136*, 10214.

(14) Mangold, S. L.; Carpenter, R. T.; Kiessling, L. L. *Org. Lett.* **2008**, *10*, 2997.

(15) Jia, F.; Lu, X.; Tan, X.; Zhang, K. *Chem. Commun.* **2015**, *51*, 7843.

(16) Tan, X.; Li, B. B.; Lu, X.; Jia, F.; Santori, C.; Menon, P.; Li, H.; Zhang, B.; Zhao, J. J.; Zhang, K. *J. Am. Chem. Soc.* **2015**, *137*, 6112.

(17) Jain, A. K.; et al. *Bioorg. Chem.* **2013**, *49*, 40.

(18) Fulda, S.; Debatin, K. M. *Oncogene* **2006**, *25*, 4798.

(19) (a) Shimazaki, K.; Urabe, M.; Monahan, J.; Ozawa, K.; Kawai, N. *Gene Ther.* **2000**, *7*, 1244. (b) Jansen, B.; Schlagbauer-Wadl, H.; Brown, B. D.; Bryan, R. N.; van Elsas, A.; Muller, M.; Wolff, K.; Eichler, H. G.; Pehamberger, H. *Nat. Med.* **1998**, *4*, 232.

(20) Watts, J. K.; Corey, D. R. *J. Pathol.* **2012**, *226*, 365.

(21) Lu, X.; Tran, T. H.; Jia, F.; Tan, X.; Davis, S.; Krishnan, S.; Amiji, M. M.; Zhang, K. *J. Am. Chem. Soc.* **2015**, *137*, 12466.

(22) Rush, A. M.; Thompson, M. P.; Tatro, E. T.; Gianneschi, N. C. *ACS Nano* **2013**, *7*, 1379.

(23) Li, Y. L.; Zhu, L.; Liu, Z.; Cheng, R.; Meng, F.; Cui, J. H.; Ji, S. J.; Zhong, Z. *Angew. Chem., Int. Ed.* **2009**, *48*, 9914.

DOI: 10.1021/jacs.6b07554
J. Am. Chem. Soc. 2016, 138, 10834−10837